HYDROLOGICAL PROCESSES
Hydrol. Process. **24**, 3661–3675 (2010)
Published online 23 July 2010 in Wiley Online Library
(wileyonlinelibrary.com) DOI: 10.1002/hyp.7804

Reconstructing the early 19th-century Waal River by means of a 2D physics-based numerical model

Alejandro Montes Arboleda,[1]* Alessandra Crosato[1,2] and Hans Middelkoop[3]

[1] *UNESCO-IHE, Department of Water Engineering, PO Box 3015, 2601 DA Delft, The Netherlands*
[2] *Delft University of Technology, Section of Hydraulic Engineering, PO Box 5048, 2600 GA Delft, The Netherlands*
[3] *Utrecht University, Faculty of Geosciences, PO Box 80·115, 3508 TC Utrecht, The Netherlands*

Abstract:

Suspended-sediment concentration data are a missing link in reconstructions of the River Waal in the early 1800s. These reconstructions serve as a basis for assessing the long-term effects of major interventions carried out between 1850 AD and the early 20th century. We used a 2D physics-based morphodynamic model accounting for the influence of floodplain vegetation to fill in this gap. Historical discharge hydrographs were derived from a correlation between flow discharge records at Cologne and water level measurements of the Rhine branches in the Netherlands, taking into account the discharge distribution between the branches. Historical floodplain sedimentation rates were estimated using old cartographic information and recent geomorphologic field work. The computed historical sedimentation rates are found to be within the range of measured data, which suggests that fine suspended sediment concentrations in the early 1800s were comparable to contemporary ones. The computations show also how vegetation enhances the formation of natural levees close to the main channel and at the same time decreases the sedimentation rates in farther areas of the floodplain. A sensitivity analysis shows suspended sediment composition to have a strong influence on the resulting quantities and patterns of floodplain deposition. The reconstruction has also provided validation of the modelling tools to reproduce the effects of vegetation on sediment dynamics, enabling their implementation to study other cases. Copyright © 2010 John Wiley & Sons, Ltd.

KEY WORDS river morphodynamic modelling; floodplain sedimentation; vegetation roughness; river reconstruction; River Waal

Received 11 September 2008; Accepted 1 June 2010

INTRODUCTION

The Rhine branches in the Netherlands have been embanked since 1000–1350 AD to protect part of the former floodplain from inundation. This confined the branches into 0·5–1·5 km wide embanked floodplains (Figure 1), predominantly used as pasture land, but also for other, often conflicting, purposes: agriculture, recreation, excavation of sand and clay, nature conservation and safety measures, all demanding space. The embanked floodplains are thus of special interest (Hesselink, 2002). The confinement of the river produced an increase of water levels and a spatial restriction of overbank deposition between the river's main channel and the embankments.

A second major intervention to the Rhine river system was the digging of the Pannerdensch Canal in 1707 AD (Figure 1), which changed the discharge distribution over the Rhine branches (Van de Ven, 1976). Near the Dutch–German border, the average discharge of the Rhine is approximately 2300 m^3/s; as the digging of the Pannerdensch Canal, the River Waal carries about 2/3 of the total Rhine discharge, with the Nederrijn and IJssel accounting for the other 1/3.

The final major intervention on the Rhine branches was the installation of a regular array of groynes approximately between 1850 AD and the early 20th century, known as the river's 'normalization'. This enhanced navigability of the channels, prevented ice clogging and accelerated drainage of high discharge peaks (Bosch and Van der Ham, 1998).

Nowadays, there is an increasing awareness that rivers need more space to safeguard flood safety under changing climatic conditions, because flood protection cannot be achieved anymore by further raising of dikes. Contemporary river management aims to increase the conveyance capacity of the rivers, allowing at the same time, but within certain bounds, natural processes of sedimentation and erosion to occur (Klijn *et al.*, 2001; Piégay *et al.*, 2005; Darby and Sear, 2008). This is done to partly restore dynamic conditions, so as to get a sustainable and more diverse river ecosystem without increasing flood levels (EU-project IRMA SPONGE at http://www.irma-sponge.org/; Baptist *et al.*, 2004; Baptist, 2005).

Measures to increase the flood conveyance capacity of the Rhine River include the lowering of the floodplains and the excavation of secondary channels. Recent restoration projects in the Netherlands successfully enhanced fluvial biodiversity (Raat, 2001; Buijse *et al.*, 2002), but there is an increasing concern over floodplain vegetation growth and its effects on the flood conveyance of the river (Villada and Crosato, 2010). Floodplain vegetation

* Correspondence to: Alejandro Montes Arboleda, UNESCO-IHE, Department of Water Engineering, PO Box 3015, 2601 DA Delft, The Netherlands. E-mail: a.crosato@unesco-ihe.org

depends on the river hydraulic regime and morphodynamics, such as the frequency of floods and the formation of new sediment deposits (Franz and Bazzaz, 1977; Hupp and Osterkamp, 1996; Johnson, 1998; Merritt and Cooper, 2000). In turn, floodplain vegetation influences the river morphodynamic trends, by locally increasing the resistance to the flow while also reducing soil erodibility (Thorne, 1990; Tsujimoto, 1999; Carollo *et al.*, 2002; Corenblit *et al.*, 2007). As a consequence, due to floodplain vegetation the flood levels increase. Finally, floodplain vegetation influences sedimentation processes (Jeffries *et al.*, 2003), ultimately resulting in a gradual rising of floodplains and reduction of the river conveyance capacity.

The extensive history of human interference makes the Rhine branches, and in the case of this study, the River Waal, an exceptionally well suited case for historical reconstructions. These reconstructions serve as a basis for assessing the long-term effects of major interventions. Also, the wealth of historic data present in the Netherlands provides an excellent opportunity to accomplish this. Notwithstanding this, available historical data do not include suspended sediment concentrations before the 20th century. We used a 2D physics-based morphodynamic model (Lesser *et al.*, 2004), together with independent estimates of historical floodplain sedimentation rates by means of geomorphologic field work, to fill in this gap.

The model accounts for the influence of floodplain vegetation on water flow, bed shear stress, sediment transport and topographic changes, distinguishing the flow between the plants and the flow above the plants, following Baptist (2005). The model can simulate sedimentation on vegetated floodplains, because it can treat the processes of fine sediment (Van Ledden, 2003).

Based on data availability, we decided to reconstruct the River Waal situation in the early 1800s, providing a basis for establishing the long-term effects of the 'normalization' works, which started in 1850 AD. Historical discharge hydrographs were derived from a correlation between flow discharge records at Cologne, Germany, and water level measurements of the Rhine branches in the Netherlands, taking into account the discharge distribution between the branches. The bed topography was derived from reconstructed cross-sectional profiles (Maas *et al.*, 1997). Historical maps of vegetation cover were derived from reconstructed ecotope maps (Maas *et al.*, 1997).

Assuming that suspended-sediment concentrations in the early 1800s were similar to contemporary ones, the computed sedimentation rates are found to be within the range of the measured data. This suggests that fine suspended sediment concentrations in the early 1800s were comparable to contemporary ones. A sensitivity analysis shows that suspended sediment composition has a strong influence on the resulting quantities and patterns of floodplain deposition. The best results are obtained for suspended sediment sizes between 16 and 30 μm. The computations show also how vegetation enhances the formation of natural levees close to the main channel and at the same time decreases the sedimentation rates in farther areas of the floodplain.

The reconstruction has provided validation of the modelling tools to reproduce the effects of vegetation on sediment dynamics and, in particular, on floodplain sedimentation rates, enabling their implementation to study other cases.

Acting as a final motivation for this study, we know that suspended sediment provides excellent binding sites for many contaminants, resulting in large amounts of contaminants being transported in particulate form to lower river reaches and their floodplains(Malmon *et al.*, 2002; Thonon, 2006). Overbank deposition may therefore not only fertilize floodplain soils, but also can cause contamination. On the timescale of years to centuries, most floodplains act as sinks for sediment and their bound pollutants (Middelkoop, 2002). The storage of these contaminants may threaten the viability of vulnerable species in the floodplain ecosystem, lead to losses in agricultural production, and if diluted, may also reach the groundwater, where they can be transported to a wider area. Thus, from an environmental point of view, the parameters that affect deposition of sediments in river floodplains merit deeper study.

STUDY AREA AND TIME PERIOD

The study area lies between the cities of Nijmegen and Tiel, along the River Waal, the largest Rhine River branch in the Netherlands. The model domain consists approximately of a 7 km long stretch of the River Waal and its embanked floodplains, in the vicinity of the towns of Slijk Ewijk, Ewijk and Winssen (Figure 1).

The site was selected due to the undisturbed nature of its floodplain soil (the land has not been excavated or mined in any way), meaning that the data collected from the field in recent years can be translated into realistic historical sedimentation rates.

The time period for the reconstruction was selected based on the following considerations: (1) Time before major human interventions and (2) Data availability. Hydrological monitoring of the lower Rhine branches in the Netherlands dates back to the late 18th century. There are no hydrological records of river flow before this time, making it very difficult to generate hydrological input data for earlier periods.

The selected period is the early 1800s. This can be considered as an optimal meeting point between the abovementioned considerations; as earlier reconstructions of the river are not feasible due to lack of hydrological input data, while a more recent baseline would be less useful for establishing the long-term effects of the 'normalization' works, which were carried out between 1850 AD and the early 20th century.

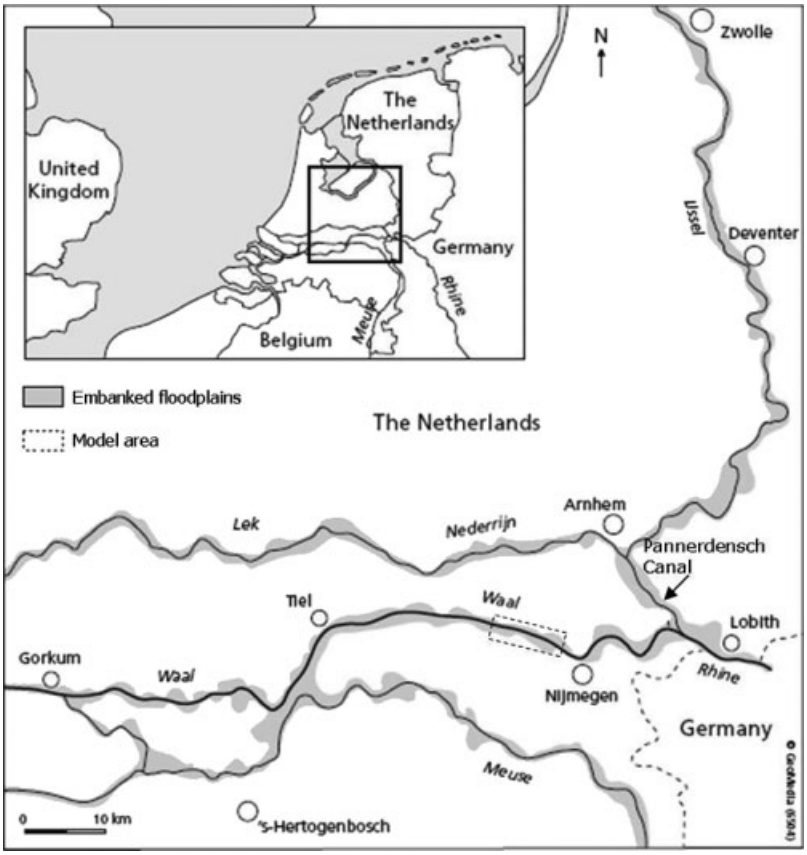

Figure 1. Location of the study area along the Waal River

MODEL DESCRIPTION

The model used for this investigation simulates non-steady flow and transport phenomena that result from meteorological forcing on a curvilinear, boundary-fitted grid. It is a fully non-linear, time-dependent, physics-based morphological model, based on the 3D Reynolds equations for incompressible fluid and shallow water (Lesser *et al*., 2004). The computations were carried out using a 2D depth-averaged version of the model with an appropriate parameterization of relevant 3D effects (Struiksma *et al*., 1985). In this case, the model accounts for two effects of the spiral motion that arises in curved flow (Blanckaert *et al*., 2002). First, the model corrects the direction of sediment transport through a modification in the direction of the bed shear stress, which would otherwise coincide with the direction of the flow velocity vector. Second, the model includes the effects of the transverse flow convection, causing a transverse redistribution of the main flow velocity, through a correction in the bed friction term. The model accounts for the effects of longitudinal and transverse bed slopes on bed load direction, accounting for gravity effects (Bagnold, 1966; Ikeda, 1982). The closure scheme for turbulence is a k-ε model, in which k is the turbulent kinetic energy and ε is the turbulent dissipation.

The effects of vegetation on hydraulic roughness are obtained by applying the method developed by Baptist (2005), conceptually similar to the one adopted by Wu *et al*. (2005). A review of methods adopted to quantify the flow resistance of vegetation in streams is provided by Corenblit *et al*. (2007). Baptist's method separates the bed shear stress from the shear stress of vegetation and distinguishes between fully and partly submerged vegetation. Plants are schematized as thin, vertical cylinders with a specified density. The resistance force is modelled as the drag force on a random or staggered array of rigid cylinders with uniform properties. The method is strictly valid for high vegetation density (Baptist *et al*., 2007) (in this context the vegetation density is high if the flow velocity can be assumed as uniform along the vertical, inside the vegetated part). The model is based on the following relation:

$$\rho g h i = \tau_b + \tau_v \tag{1}$$

where ρ is the mass density of water (kg/m^3); g is the acceleration due to gravity (m/s^2); h is the water depth (m); i is the longitudinal water surface slope (−); τ_b is the bed shear stress (N/m^2) and τ_v is the shear stress caused by vegetation (N/m^2).

Partly submerged vegetation

In the case of uniform flow through partly submerged vegetation, the water depth is smaller than the height of plants and the flow velocity through the plants coincides with the reach-averaged velocity. In this case:

$$\tau_b = \frac{\rho g}{C_b^2} u_c^2 = \frac{\rho g}{C_b^2} \overline{u}^2 \tag{2}$$

and

$$\tau_v = \frac{1}{2}\rho C_D m D h u_c^2 = \frac{1}{2}\rho C_D m D h \overline{u}^2 \quad (3)$$

in which C_b is the bed roughness expressed by the Chézy coefficient ($m^{1/2}/s$); u_c is the flow velocity through vegetation (m/s); $\overline{u}$ is the reach-averaged value of flow velocity (m/s); m is the cylinder density per unit area ($1/m^2$); D is the cylinder diameter (m) and C_D is the drag coefficient associated with the vegetation type (−), estimated in an empirical way with values varying between 1 and 2 (Stolker and Verheij, 2000).

For partly submerged vegetation the flow can be described by the following Chézy relation:

$$\overline{u} = C_r\sqrt{hi} \quad (4)$$

where C_r is the representative roughness of the partly submerged vegetation ($m^{1/2}/s$), which, by combining Equations (2) and (3) and taking into account that $u_c = \overline{u}$, is given by:

$$C_r = \sqrt{\frac{1}{\frac{1}{C_b^2} + \frac{C_D m D h}{2g}}} \quad (5)$$

Fully submerged vegetation

For fully submerged vegetation the water depth is larger than the height of plants. In this case it is assumed that the flow velocity is uniform between the plants (Wilson *et al*., 2003), but has a logarithmic profile above them, starting from the value u_c, which is given by (elaborations in Baptist, 2005):

$$u_c = \sqrt{\frac{1}{\frac{1}{C_b^2} + \frac{C_D m D k}{2g}}}\sqrt{hi} \quad (6)$$

where k is the height of plants (m).

In the case of fully submerged vegetation:

$$\tau_b = \frac{\rho g}{C_b'^2}\overline{u}^2 \quad (7)$$

where:

$$C_b' = C_b + \frac{\sqrt{g}}{\kappa}\sqrt{1 + \frac{C_D m D k C_b^2}{2g}}\ln\left(\frac{h}{k}\right) \quad (8)$$

in which κ is the Von Kármán constant ($\kappa = 0{\cdot}4$).

As for the previous case, for the flow through and over-submerged vegetation the process can be described by a Chézy relation:

$$\overline{u} = C_{rs}\sqrt{hi} \quad (9)$$

where:

$$C_{rs} = \sqrt{\frac{1}{\frac{1}{C_b^2} + \frac{C_D m D k}{2g}}} + \frac{\sqrt{g}}{\kappa}\ln\left(\frac{h}{k}\right) \quad (10)$$

Note that when $h = k$, C_{rs} (Equation (10)) equals the representative roughness for non-submerged vegetation C_r (Equation (5)). For $h > k$, the value of C_{rs} is larger than the value of C_r, which means that fully submerged vegetation offers smaller resistance to flow than partly submerged vegetation.

Baptist *et al*. (2005) and Facchini *et al*. (2009) tested the performance of this modelling tool in reproducing the effects of different types of vegetation on water flow, sediment transport and floodplain sedimentation. Baptist *et al*. applied the vegetation model to the rivers Rhine (The Netherlands), Volga (Russia) and Allier (France). In the latter case, the results were compared to the data collected in the field before and after a flood event, with the conclusion that the model gave reliable results. In particular, the model did not overestimate floodplain erosion as 'classical' methods, based on simply imposing higher roughness to vegetated areas, do. When applying the methodology to real rivers, the major difficulty in using this model was found to be the schematization of real plants in terms of height diameter and density. This was later carried out by Baptist (2005) for several vegetation types.

Facchini *et al*. (2009) applied the model to simulate the present trends of floodplain sedimentation along the Waal River near Ewijk, at a location inside the present study area. For every vegetation type, they used the characteristics that were suggested by Baptist (2005). The results were validated with field data carried out over a period of 10 years. The computed sedimentation rates agreed with the measured ones also in their spatial variability.

Crosato and Samir-Saleh (submitted) found that the model overestimates the resistance offered by the plants for low vegetation densities (approximately <10 stems/m^2). This is due to the assumptions of rigid stems and uniform flow velocity between the plants.

MODEL SETUP

Curvilinear grid and bed topography

In Maas *et al*. (1997), a copy of an old river map and a set of 17 reconstructed cross-sectional profiles were used to construct a 1D model of the Waal River. The map corresponds to the study area selected for this research and is originally from the year 1800 AD, which made it suitable for our model build up. An indication of the quality of the available information is shown in Figure 2. The embankments and the locations of the 17 cross sections were digitized from the map.

The curvilinear grid follows the alignment of the main channel with the embankments being used as land boundaries (cells lying outside of the boundary were deleted to avoid unnecessary computations). The modelled stretch is 7 km long and 1 km wide on average (the width of the main channel is approximately 400 m). The mean grid cell size is 50 m, allowing a sufficient

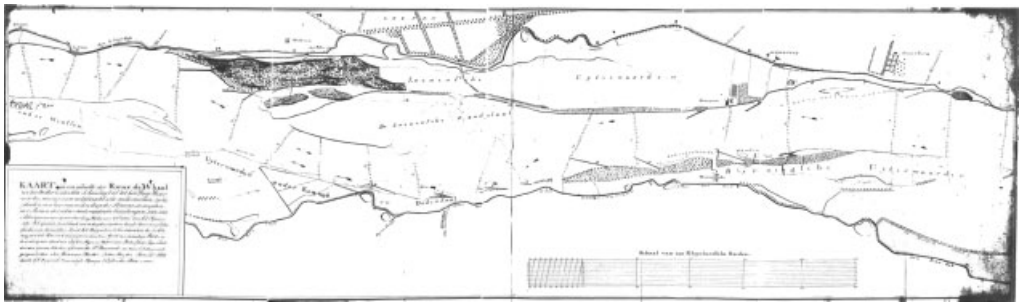

Figure 2. Old map of the Waal River (1800 AD) showing the study area and the (poor) quality of the historical cartographic information available

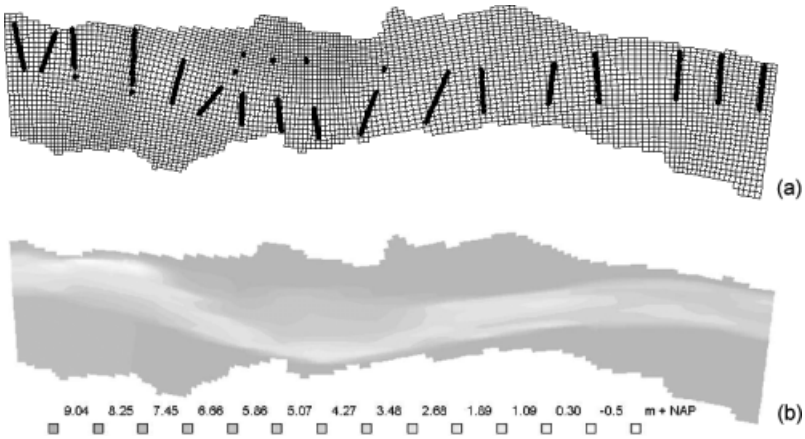

Figure 3. (a) Curvilinear grid with the location of cross-sectional profiles and (b) resulting bed topography

amount of data points along the cross section with a reasonable computational time.

To generate the model bed topography, water depth points from the cross-sectional profiles were translated into bed levels; in the areas between successive cross sections the bed levels where derived by interpolation, the streamwise distance between successive cross sections being approximately 400 m. Topographical information of the floodplains was not available, so they were schematized as horizontal surfaces with a longitudinal slope equal to the bankfull level slope (Figure 3). This approximation is a strong limitation of the model, because the present differences in elevation of the Waal floodplains can reach 3–4 m (Middelkoop and Asselman, 1998).

It is important to mention that, although sediment transport is computed for every time step, the bed topography was not updated during the simulation period (i.e. the model has a fixed bed). The averaged historical floodplain sedimentation rates (see Section on Estimates of Sedimentation Rates from the Field) were found in the order of 5–16 mm/year, corresponding to floodplain rises between 10 and 30 cm in 20 years. The uncertainty related to not taking into account the effects of this rise on sedimentation rates is therefore much smaller than the uncertainty related to assuming that the floodplains were horizontal surfaces.

Fixing the main channel bed was mainly due to lack of data on riverbed topography for the successive 50 years, which made it impossible to calibrate and validate the model on the prediction of riverbed evolution. From the observation of an historical map of 1819 AD (Cadastral Map of the Municipalities of Loenen and Wolferen), there is no evidence of any severe changes in the main river channel alignment and on bar development in the study area for about 20 years. As this research concentrates on the river floodplains, assuming a fixed main-channel riverbed can be considered an acceptable simplification. The major consequence lies in the uncertainty related to the flow velocity distribution in the main channel, which could change with time influencing the sedimentation rates on the floodplains near the main channel margin. However, farther from the main channel, flow velocity and sediment transport rates are governed by the local roughness and floodplain topography.

Flow discharges

For several gauging stations along the lower river Rhine branches, records of daily water levels are available since 1770. Unfortunately, flow discharge records are scarcer. Complete discharge records are only available from 1817 at Cologne, upstream of the Dutch–German border. However, correlations between water levels downstream of the border and flow discharges at Cologne have been developed in recent years, in order to reconstruct flow discharges prior to this date.

Van Vuuren (2005) studied the relationship between water levels at Arnhem and flow discharges at Cologne for the period 1816–1821. The distance between Cologne and Arnhem along the River Rhine is 200 km. In this

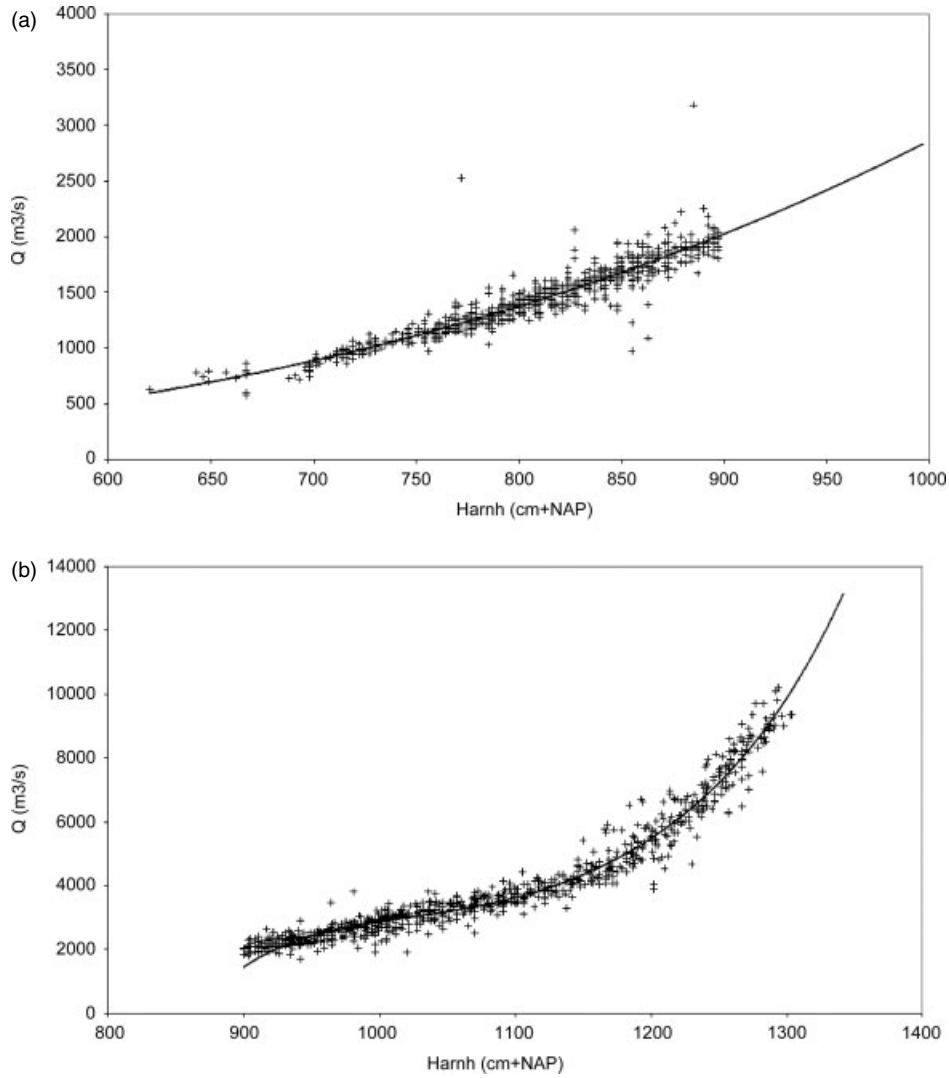

Figure 4. QH-relationship: Q-Cologne—H-Arnhem for the period 1816–1821 with (a) valid for H-Arnhem <900 (cm+NAP) and (b) valid for H-Arnhem >900 (cm+NAP) (Van Vuuren, 2005)

river reach, the major tributary is the Ruhr (218 km long, average discharge 79 m^3/s), joining the Rhine near Duisburg, at an elevation of 17 m above sea level.

By considering time lags between data points, Vuuren developed a set of rating curves that could be used by us to reconstruct Rhine discharges from the year 1770 (Figure 4). These rating curves were used to reconstruct a series of river discharges at Cologne for the period 1790–1810, from a complete series of water levels at Arnhem. The discharge values at Cologne were then used as a base to generate a series of flow discharges for the Waal River to be used as input to the model. The following considerations were taken into account during the process:

1. The catchment area of the River Rhine at the Dutch–German border, just upstream of the bifurcation that forms the Dutch Rhine branches, is 11% larger than the catchment area at Cologne.
2. The River Waal carries 2/3 of the total Rhine discharge after the bifurcation (Hesselink *et al.*, 2006).

According to this, a reasonable estimate of the Waal discharge from a known discharge value at Cologne can be defined by:

$$Q_{\text{Waal}} \cong \frac{2}{3}\left(Q_{\text{Cologne}} \times 1{\cdot}11\right) \tag{11}$$

This relationship was used to generate a series of Waal river discharges for the period 1790–1810. Three 'typical' hydrological years were extracted from the generated series: low-range, mid-range and high-range, as suggested by Asselman and Middelkoop (1998). To select the most appropriate years to be representative of the entire period, the 21 yearly hydrographs were ordered according to flood magnitude. They were then separated into the three classes with the central year in each class selected for modelling. The selected hydrographs correspond to the hydrological years of 1790–1791 (mid-range flood), with discharges between 1000 and 4700 m^3/s, 1793–1794 (low-range flood), with discharges between 750 and 3050 m^3/s and 1804–1805 (high-range flood), with discharges between 1500 and 6400 m^3/s (Figure 5).

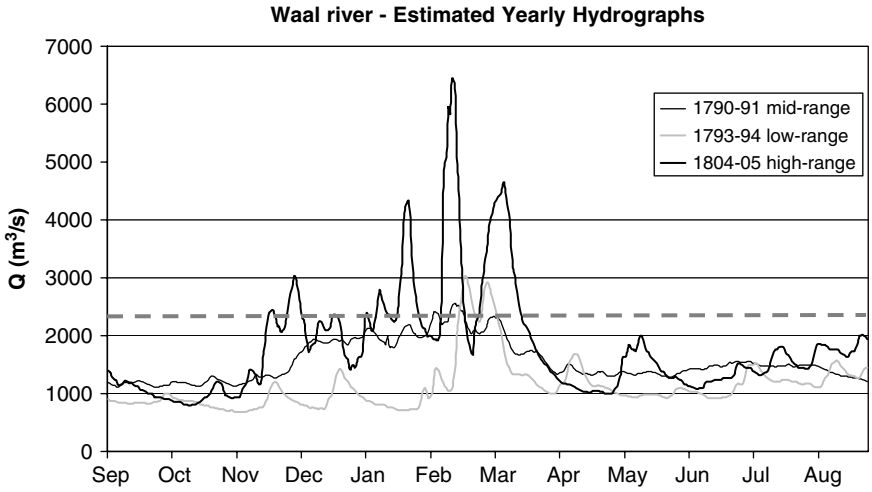

Figure 5. Estimated Waal River discharges for the period 1790–1810: low-, mid- and high-range annual hydrographs. Dotted grey line: bankfull discharge (2350 m^3/s)

Main channel bed roughness

The data extracted from Maas *et al.* (1997) for a previously constructed 1D model of the Waal River, served as the starting point to determine a Chézy bed roughness coefficient for the main river channel in our model. The mentioned 1D model was built to represent the same period that we attempted to represent with this model and a Chézy bed roughness coefficient C = 45 $m^{1/2}/s$ was adopted in that time.

Maas *et al.* (1997) suggested a value Q = 2350 m^3/s for the Waal River, that could be assumed as representative of the bankfull discharge for the given period. This value has been used to run short period simulations with uniform discharge (until equilibrium conditions were reached) to determine the most suitable bed roughness coefficient for our model.

The results of the calibration procedure show that with a value of C = 50 $m^{1/2}/s$, the water levels in the model are closer to bankfull levels. From this, it was clear that this higher value of C was more appropriate to represent the main channel bed roughness in our 2D model.

Main channel bed material

Even though the major part of the suspended load of the Rhine River consists of silt and clay-sized material (Middelkoop, 1997), fractions of the sandy bed may also be suspended depending on the local flow velocities, and thus may be deposited on the river floodplains during overbank flow events. To account for this, a sand bed layer had to be defined in the model.

Median grain sizes of the sand bed material along the Wall River were determined to be around 850–1000 μm during the early 1800s by Maas *et al.* (1997). A value of D_{50} = 900 μm was adopted for the present model.

Suspended sediment input from upstream

The average relation between discharge and suspended sediment concentrations is described by a rating curve. Using a record of daily discharges and suspended sediment concentrations of the River Rhine at the Dutch–German border measured in the period 1970–1990, Asselman (1997) constructed a sediment rating curve in the form of a power function. The sediment rating curve for the Waal River (Figure 6) was constructed based on the one generated by Asselman (1997) for the Rhine at the Dutch–German border.

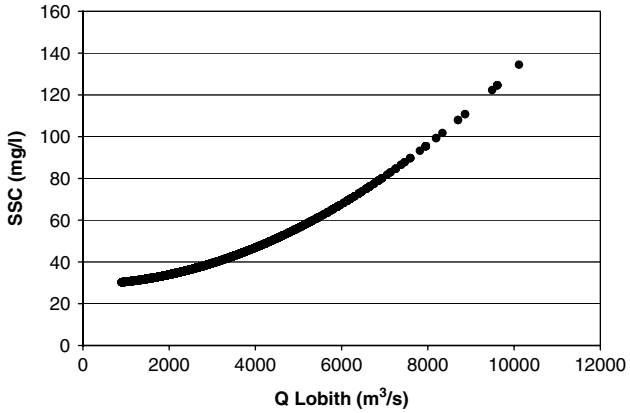

Figure 6. Suspended sediment rating curve for the Waal River (Asselman, 1997)

Asselman's rating curve is based on contemporary discharge and suspended sediment concentration data. However, sediment data for earlier periods are not available, so the curve has been adopted for the model based on the assumption that the relationship between discharge and suspended-sediment concentration has not suffered significant changes in recent time. Assuming that, in the early 1800s, the suspended sediment concentrations were similar to contemporary ones seemed appropriate. Although recent river interventions, such as dams in the upstream reaches, may have decreased suspended sediment concentrations, at the same time the progressive reduction of floodplain size all along the water course increased the suspended sediment concentrations in the flowing water (lower sedimentation rates due to higher velocities). The similarity between sediment

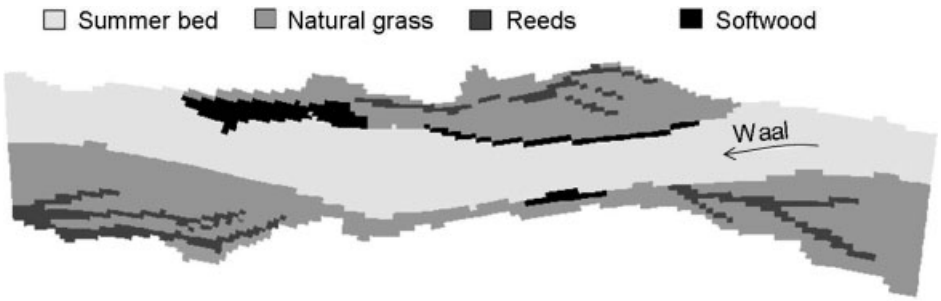

Figure 7. Spatially varying vegetation cover according to historical ecotope maps

Table I. Selected vegetation types from typical floodplain vegetation (Van Velzen *et al*., 2003)

Vegetation type	Diameter (m)	Density (m^{-2})	Height (m)	Drag coefficient (−)
Natural grass	0·003	4000	0·1	1·8
Reed	0·0046	80	2·5	1·8
Softwood	0·14	0·2	10·0	1·5

concentrations in the early 1800s and contemporary ones formed the main hypothesis we tested using the developed model.

In the model, the suspended sediment that enters the domain at the upstream boundary is characterized by its fall velocity. Assuming that the type of sediment has not significantly changed with time, the fall velocity was set to 0·1 mm/s, which is characteristic of silt particles having a diameter, D, of 16 μm.

Floodplain vegetation

Vegetation cover data was extracted from ecotope maps of the study area that were reconstructed by Maas *et al*. (1997) between the years 1780 and 1830.

The area was mostly covered by natural grasslands, with some influence of reed that grows in old traces of secondary channels and softwood shrubs and forest that protect the banks.

Spatially varying vegetation was schematized by assigning index values to each floodplain cell, according to the vegetation type (Figure 7). Specific vegetation parameters were assigned to each index value (diameter, height, density and drag coefficient as specified in Table I) to calculate the representative roughness of the vegetation (following the method developed by Baptist, 2005).

RESULTS

Simulations on the constructed model were carried out for three different hydrological years (1790–1791, 1793–1794 and 1804–1805) and considering two scenarios: (1) no vegetation on the floodplains and (2) with spatially varying floodplain vegetation according to the historical ecotope maps.

In the modelled stretch, it is possible to identify three main floodplain sections; one colliding with the upstream boundary (close to the city of Nijmegen), another one close to the downstream boundary (next to the town of Winssen) and one in the central part of the model, located on the right bank and close to the town of Slijk Ewijk. To avoid results that are influenced by boundary disturbances, the analysis was carried out for the central floodplain area only (Figure 8).

It is also important to mention that, although sand bed material transport was also modelled, the results presented in the upcoming section consider the deposition of fine suspended sediment ($D < 63$ μm) only. Deposition of suspended sand bed material resulted in natural levee formation close to the main channel margin. Farther from the main channel, sand deposition was not significant compared to deposition of fine sediment (Figure 9). These results are confirmed by field data (Middelkoop, 1997) showing that 63% of the material forming the natural levees along the Waal River close to the study area is sand having grain size smaller than 2 mm and 37% silt and clay. Instead, 40% of the sediment settling in the central part of the River Waal floodplains has grain size smaller than 2 μm (clay), 57% between 2 and 32 μm (silt), whereas only 3% has diameter larger than 32 μm (silt and sand).

Deposition of fine suspended sediment

Figure 10 presents the results of annual fine sediment deposition rates (kg/m^2) for the different scenarios considered. The plots on the left represent the scenario without floodplain vegetation while the ones on the right show results for the scenario with spatially varying vegetation. Each pair of plots is presented with a fixed scale for comparison purposes.

In general, the plots show high accumulation of fine sediment close to the river channel with a gradual decrease in deposition as we move farther away from the river bank.

Overall sedimentation is 20% higher in the case with no vegetation. Also, the deposition pattern is quite homogeneous in the longitudinal direction, contrary to the case considering floodplain vegetation, where distinct spatial patterns can be identified as a result of flow across and over vegetation, with higher deposition over grasslands compared to areas covered with taller reed.

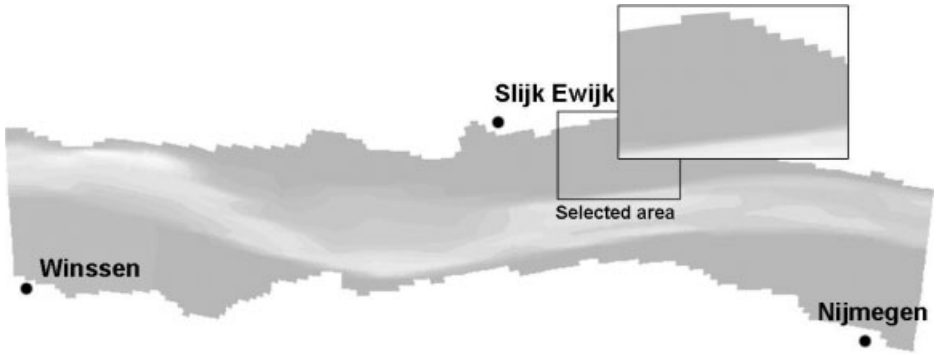

Figure 8. Detail of selected floodplain section. The rectangle encloses the area for which results are analysed

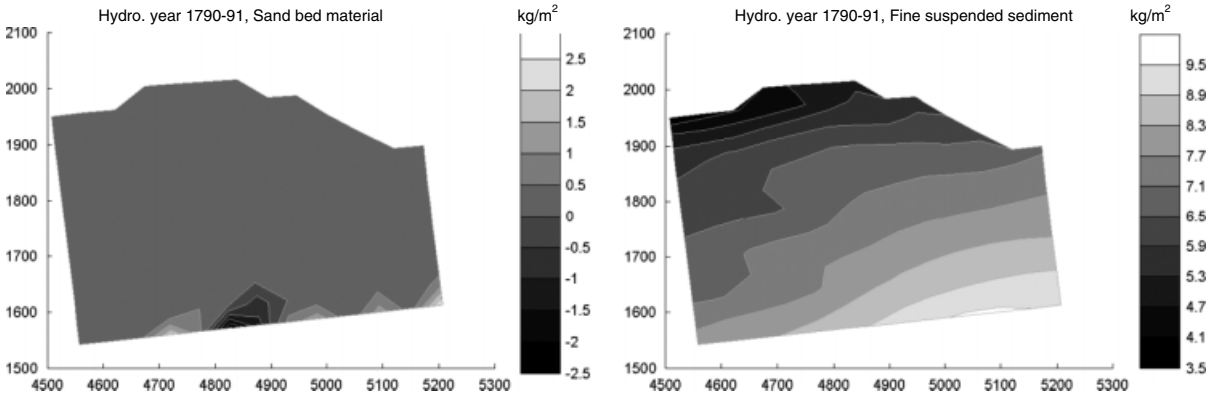

Figure 9. Deposition of sand bed material compared to deposition of fine sediment on the selected floodplain area. Left: sand ($D = 900$ μm), negative values correspond to erosion. Right: fine material ($\omega_S = 0{\cdot}1$ mm/s; $D = 16$ μm)

Table II presents a synthesis of the quantitative results for fine suspended sediment deposition obtained after the modelling phase. The translation of annual sediment deposition (kg/m^2) to an equivalent sediment depth (mm) was done by dividing deposition values by a representative value of dry bed density (kg/m^3). A value of 800 kg/m^3, representative of the fine sediment that can be encountered in the Waal floodplains, was adopted for the conversion (John Cornelisse, Deltares, personal communication).

The computed averaged annual floodplain sedimentation of fine material for the period 1790–1811, with the vegetation cover of the time, ranges between 5·1 and 10·8 kg/m^2, corresponding to 6·3–13·5 mm/year.

Depth-averaged velocities

Figure 11 shows depth-averaged velocities (m/s) during peak discharge for the selected floodplain section. The plot area was extended to include the main channel of the river in order to appreciate the effect of flow concentration. The plots on the left represent the scenario without floodplain vegetation while the ones on the right show results for the scenario with spatially varying vegetation. Each pair of plots is presented with a fixed scale for comparison purposes.

The plots clearly show the effect of flow concentration exerted by floodplain vegetation. The increased resistance reduces flow over the floodplain and enhances main channel flow. This effect is also visible locally within the floodplain due to the spatially variable vegetation.

Suspended sediment concentrations

Figure 12 presents concentration values of fine suspended sediment (kg/m^3) during peak discharge for the scenarios considered. The plots are presented in the same way as for the previous variables.

Similarly to the flow velocity results, it is possible to observe the effects of flow reduction over the vegetated areas and flow enhancement over the less-resistant areas, translated into lower suspended sediment concentrations over the floodplains with a tendency to be higher towards the river main channel. We can also see how the relative differences between the two scenarios are more evident in low flooding conditions compared to higher discharge conditions, where flow is less concentrated towards the main channel and more uniform suspended sediment concentrations are observed over the plotted area.

ESTIMATES OF SEDIMENTATION RATES FROM THE FIELD

An independent estimation of the average floodplain sedimentation rates was carried out using old cartographic information in combination with recent geomorphologic field work in order to validate the model results (Middelkoop, 2002).

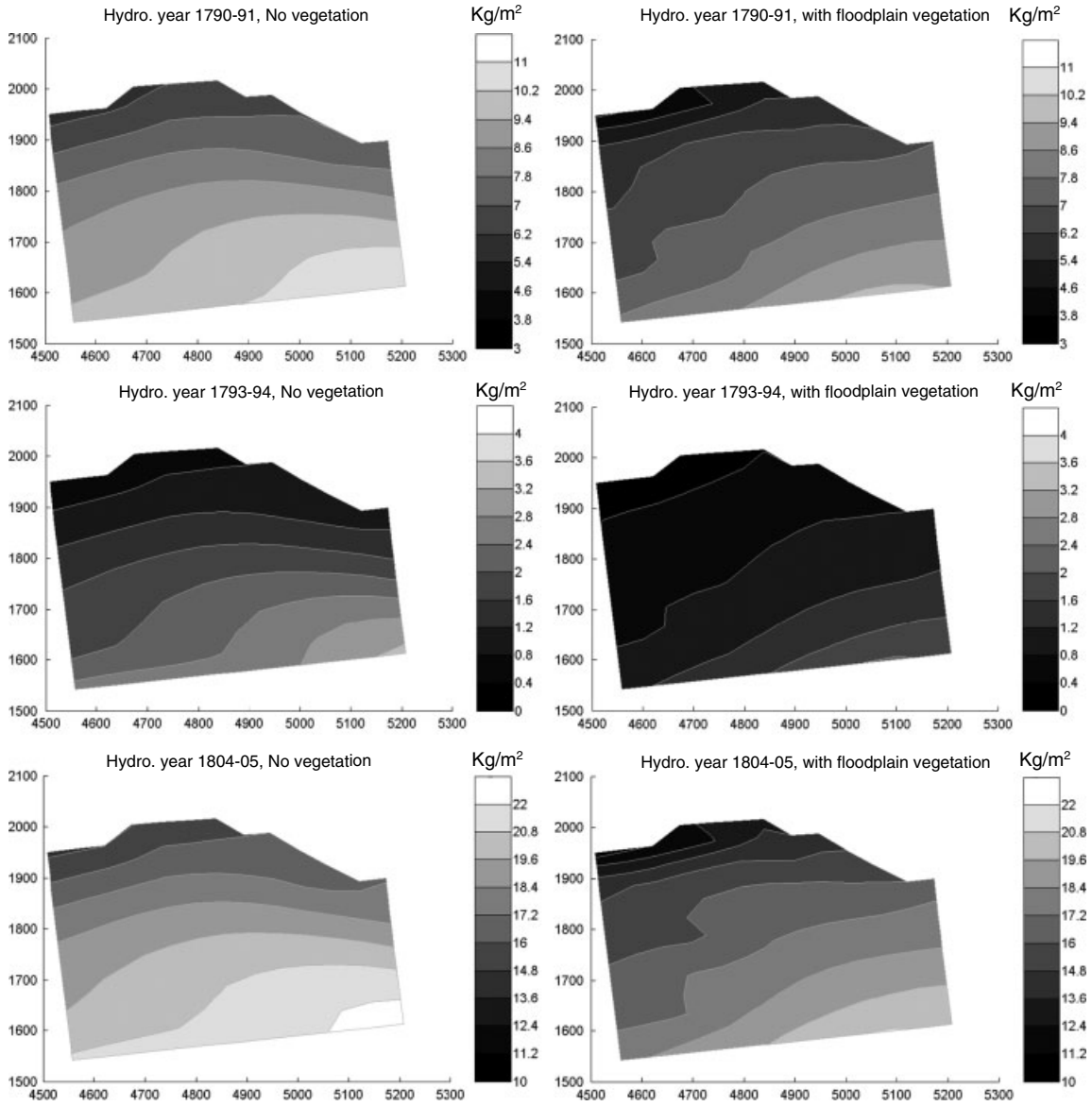

Figure 10. Computed deposition rates of fine suspended sediment on the selected floodplain area. Note that the colour bars have different scales

Table II. Floodplain sedimentation rates on the selected area

Hydrological year	Fine sediment deposition rate (kg/m^2)/ year		Sedimentation rate (mm/year)	
	Without floodplain vegetation	With floodplain vegetation	Without floodplain vegetation	With floodplain vegetation
1790–1791 (1)	6·0–11·0	4·0–9·5	7·5–13·8	5·0–11·8
1793–1794 (2)	0·5–3·5	0·2–2·0	0·6–4·4	0·3–2·5
1804–1805 (3)	15·0–22·0	11·0–21·0	18·8–27·5	13·8–26·3
Average for the period	7·2–12·2	5·1–10·8	9·0–15·2	6·3–13·5*

(1) mid-range flooding; (2) low-range flooding; (3) high-range flooding.
* Observed: 5–16 mm/year.

Old river maps provide an indication of the beginning of overbank sedimentation on a newly formed bench. The total thickness of overbank deposits on a sand bar can be determined by means of coring. Dividing the total sediment accumulation by the number of years of sedimentation since the formation of the bench yields a rough indication of the average sedimentation rate on the floodplain section. For this procedure to be valid, the floodplain section must be undisturbed (e.g. not affected by clay digging), which is in fact the case for our selected floodplain section.

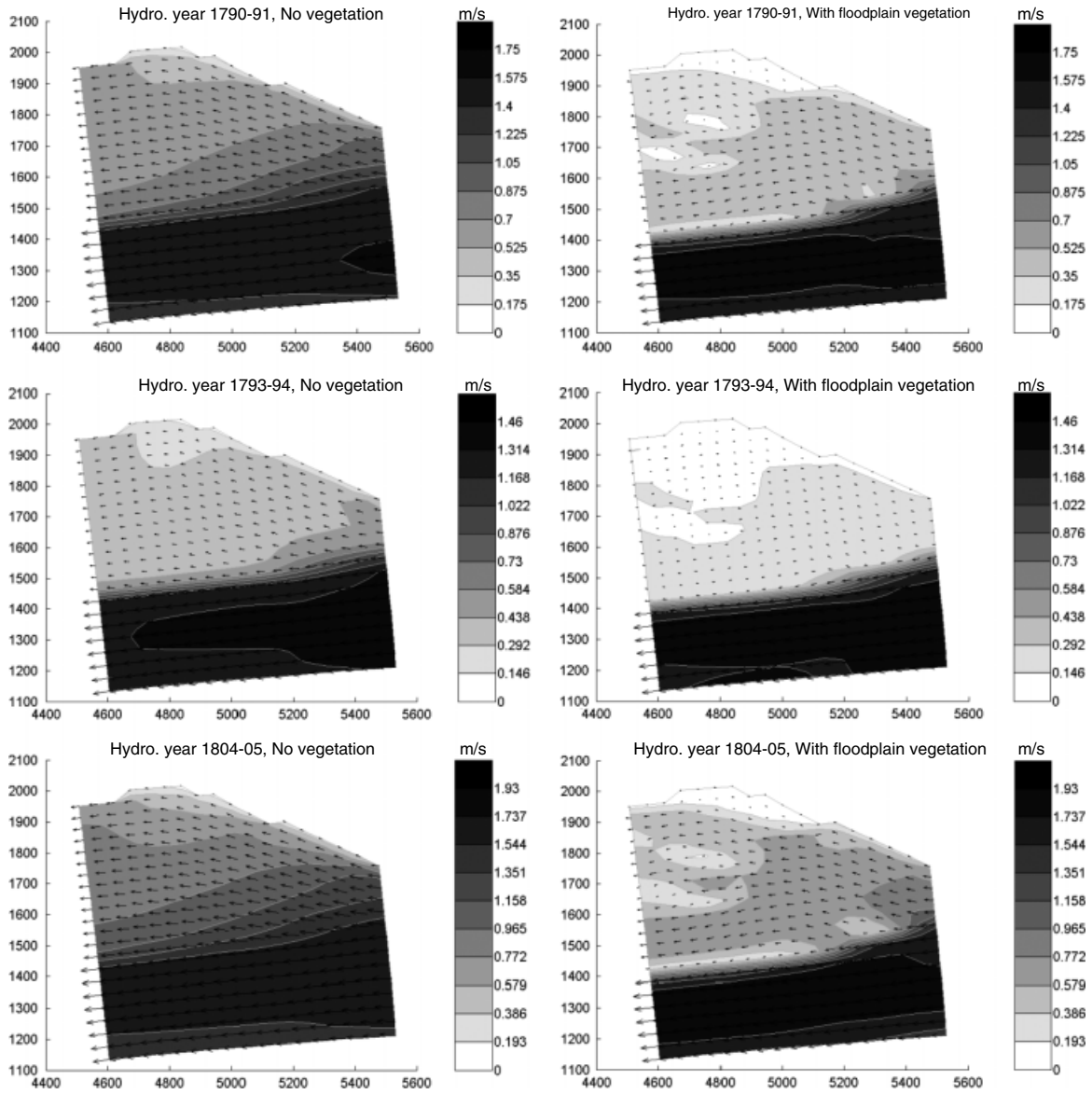

Figure 11. Computed depth-averaged velocities during peak discharge in the selected floodplain area and adjacent channel. Note that the colour bars have different scales

Following this procedure, it was determined that the average sedimentation rates of silt and clay in the studied site since the beginning of overbank deposition, are in the order of 5–16 mm/year (averaged over time intervals of more than a century). Considering a bed density of 800 kg/m^3 this corresponds to averaged annual sedimentation rates of 4·0–12·8 kg/m^2.

For comparison, Middelkoop and Asselman (1998) estimated that the amounts of silt- and clay-sized sediment deposited during the high-magnitude flood event of December 1993 ranged between 1·2 and 4·0 kg/m^2, corresponding to 1·5–5·0 mm of bed level rise during one single high-magnitude event.

SENSITIVITY ANALYSIS

There is a lack of detailed information regarding the grain sizes of fine suspended sediments in the River Waal, whereas this is a necessary information for the upstream boundary of the model. For modelling purposes a uniform sediment type was used, although this is hardly the case in reality.

A sensitivity analysis was carried out to determine the influence of varying sediment types on floodplain sedimentation (by experimenting with different values of the settling velocity). In this research, a value of $\omega_S = 0{\cdot}1$ mm/s ($D = 16$ μm) was adopted. Additional simulations were performed for the mid-range hydrological year (1790–1791) with $\omega_S = 0{\cdot}05$ mm/s ($D = 8$–16 μm) and $\omega_S = 0{\cdot}2$ mm/s ($D = 16$–30 μm). The results are presented in Figure 13. These results can be compared to the measured annual (averaged) sedimentation rates of 4–12·8 kg/m^2. Realistic sedimentation rates are obtained for both $\omega_S = 0{\cdot}1$ mm/s and $\omega_S = 0{\cdot}2$ mm/s (suspended sediment having diameter of 16 μm or between 16 and 30 μm). Considering that during high-range hydrological years the sedimentation rates are higher, the best

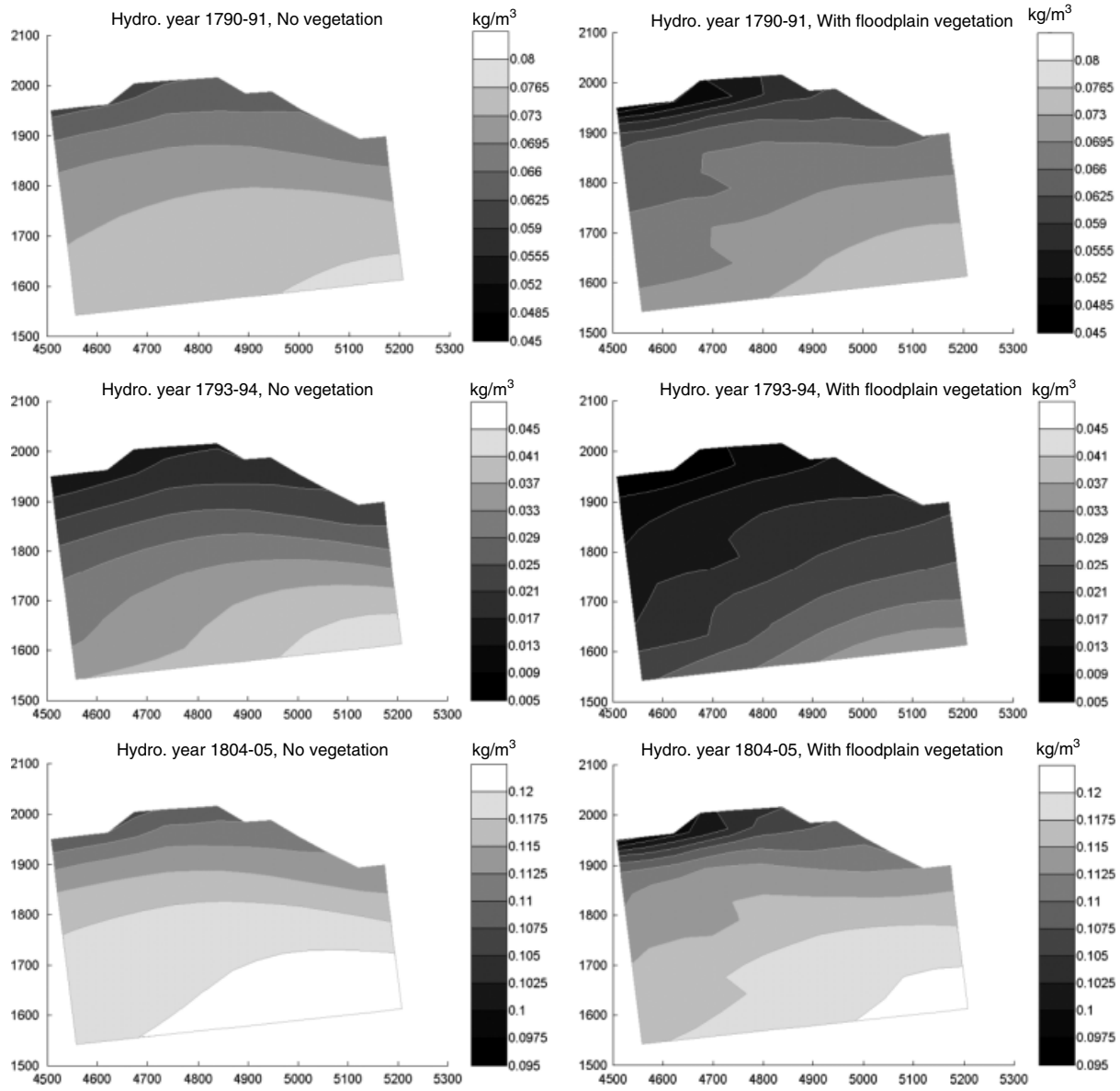

Figure 12. Computed concentrations of fine suspended sediment during peak discharges in the selected floodplain area. Note that the colour bars have different scales

long-term predictions are obtained for $\omega_S = 0{\cdot}1$ mm/s ($D = 16$ μm).

The plotted results show that sedimentation rates and patterns are sensitive to variations in sediment type. Deposition rates considerably increase when considering a higher settling velocity. In terms of distribution of the deposition rates on the floodplain area, relative differences are also much more significant with higher settling velocities, while smaller velocities result in a much more uniform distribution of the sediment.

Suspended sediment data collected by Asselman (1997) show no long-term trends of suspended sediment concentrations, for this reason and considering the balance of changes that occurred in the river (see Section on Model Setup), we have assumed that relations between concentration and discharge were more or less the same in the early 19th century. This assumption is supported by the results, as the computed sedimentation rates fall within the measured range. Instead, a strong uncertainty is related to the sediment size. For this reason, we have focused our sensitivity analysis on the settling velocity (dependent on sediment size), as described above. However, we can also consider the results as representative of the influence of varying the sediment concentration at the upstream boundary. This assumption is based on the following considerations.

For the local sedimentation rates

We can derive the sedimentation rates from the one-dimensional sediment mass balance for a river with suspended sediment transport (bed load transport is not significant, as in our case study):

$$-c_a\omega_S - E = \frac{\partial z_b}{\partial t} \tag{12}$$

where c_a is the sediment concentration at point a, point on the vertical close to the river bed (−) (in the model we

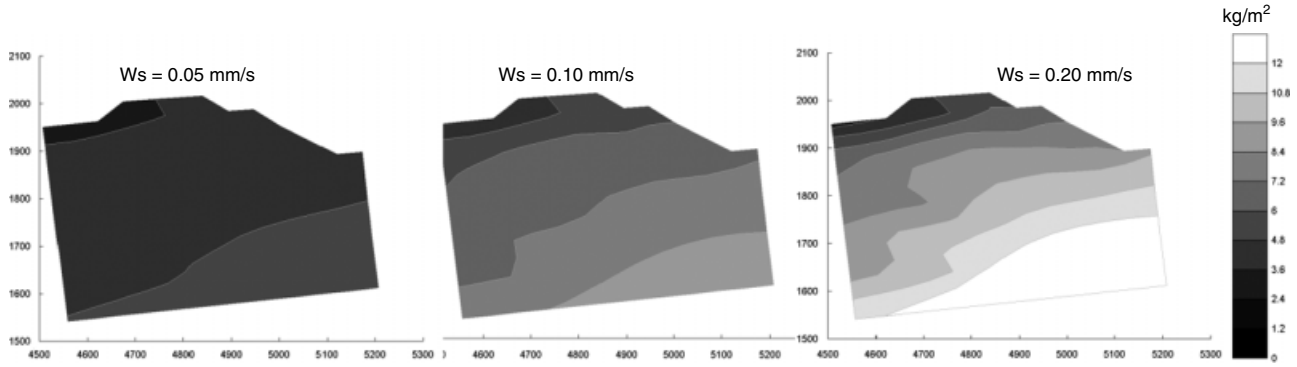

Figure 13. Sensitivity analysis: influence of fine sediment size on floodplain sedimentation pattern and rates. Computations were carried out for the mid-range hydrological year 1790–1791 (measured averaged annual sedimentation rates between 4·0 and 12·8 kg/m^2)

used depth-averaged sediment concentrations); ω_S is the settling velocity of sediment particles, positive downward (m/s); E is the sediment entrainment rate per unit of bed surface (m/s); z_b is the local bed level (m) and t is time (s).

The entrainment of sediment from the bed, E, is a function of the local bed shear stress, which is only weakly dependent on the quantity of sediment in suspension (only for high sediment concentrations there is a dependency, but this is not the case of the Waal River). For this reason, the sediment concentration affects the sedimentation rate, $\frac{\partial z_b}{\partial t}$ (positive upward), only through the product concentration × settling velocity: $c_a\omega_S$.

For temporal and spatial variations of floodplain sedimentation rates

The water flow is not influenced by sediment concentrations for the values of concentrations that are characteristic of the Waal River. The model that we used is 2D depth-averaged and adopts the method developed by Galappatti (1983) (see also Galappatti and Vreugdenhil, 1985), describing the spatial and temporal variations of depth-averaged suspended load. According to this method the first-order form of the equation for the depth-averaged concentration can be written as:

$$c(t) + T\frac{\mathrm{d}c}{\mathrm{d}t} = c_e(t) \tag{13}$$

The solution is:

$$c(t) = c_e(t) - [c_e(t) - c(0)]\exp(-t/T) \tag{14}$$

To see the behaviour of this equation consider the case in which the equilibrium concentration $c_e = 0$:

$$c(t) = c(0)\exp(-t/T) \tag{15}$$

with the temporal scale:

$$T = \frac{\gamma_1}{\gamma_0}\frac{h}{\omega_S} \tag{16}$$

in which

$$\frac{\gamma_1}{\gamma_0} = f\left(\frac{\omega_S}{u_*}, \frac{u}{u_*}, \frac{z_b}{h}\right) \tag{17}$$

where h is the water depth (m); u_* is the shear velocity (m/s); u is the flow velocity (m/s); $c(0)$ is the concentration at $t = 0$ and γ_0 and γ_1 are shape factors, not dependent on concentration.

The temporal scale T is not a function of sediment concentration. A similar result can be found for the spatial scale. Therefore, initial and upstream concentrations have no influence on the temporal and spatial scales of sediment concentrations. From the solution of the equation we can observe that $c(t)$ is linearly proportional to $c(0)$ (initial or upstream concentration respectively, if we deal with either temporal or spatial variations).

The sedimentation pattern does not change with $c(0)$, but the bed level changes do and are linearly proportional to $c(0)$. The pattern of sedimentation is given by the value of the settling velocity and by the hydrodynamic conditions (u, h, u_*), which do not change with the concentration values present in the Waal River. It was therefore more interesting to study, with this model, the influence of varying sediment grain sizes (through the settling velocity) on sedimentation rates, because changes of upstream concentrations lead to the same sedimentation pattern and to sedimentations rates that are proportional to the input sediment concentrations.

CONCLUSIONS AND DISCUSSION

With the assumption that suspended sediment concentrations in the early 1800s were similar to contemporary ones, the floodplain sedimentation rates resulting from the model fall within the range of values estimated from old cartographic information and field work. The computed values range between 6·3 and 13·5 mm/year; the ones derived from geomorphologic field work between 5 and 16 mm/year (Table II). The agreement between computed and measured annual sedimentation rates on the Waal floodplains suggests that suspended sediment concentrations have not changed much during the last 200 years. This is probably due to counterbalancing effects of the interventions carried out along the Rhine River since the 1800s. Although dams in the upstream reaches may have decreased suspended sediment concentrations, at the same time the progressive reduction of

floodplain size all along the water course increased the suspended sediment concentrations in the flowing water (lower sedimentation rates on floodplains due to higher velocities). We have to admit, however, that the validation data are poor, because they are the result of averaging over a long period of time.

The general spatial variations of floodplain sedimentation observed from the simulations show larger quantities of deposition close to the main channel with a gradual reduction in deposition towards farther parts of the floodplain area. This is evidence of the diffusive transport of suspended sediment from the main channel to the floodplains (concepts on sediment transport mechanisms during overbank flow events can be found in Pizzuto, 1987). This pattern is much more pronounced after lower-range floods. Deposition patterns resulting from larger floods are more uniform, with sediment carried further into the floodplain (evidence of joint diffusive and convective transport).

Results after introducing floodplain vegetation show even less sedimentation over the farther areas of the floodplain with most of the sediment depositing close to the main channel. The increased flow resistance exerted by the vegetation concentrates the water flow in the main channel and reduces flow velocity as well as sediment concentration over the floodplain. Even though the reduction of flow velocities enhances conditions for sediment deposition, there is considerably less sediment flowing over the floodplain, hence less sediment available for deposition, especially over the farther areas of the floodplain.

A similar approach can be taken to explain local deposition patterns resulting from the simulation of spatially variable vegetation. The results show larger accumulation of sediment over the grassland areas compared to areas covered by reed. With water flowing over the spatially variable vegetation, the larger flow resistance exerted by reed, enhances flow over the less resistant grasslands, resulting in larger sediment concentrations over this area; hence, more sediment available for deposition. In general, model results agree qualitatively with recent observations on spatial variations of sedimentation on the Waal and Meuse floodplains (Middelkoop and Asselman, 1998) and with the field observations of Jeffries *et al*. (2003) on the Highland Water Stream (England).

Results from the sensitivity analysis show a significant influence of sediment type on resulting rates and patterns of floodplain sedimentation. The size of suspended sediment may affect the relative importance of diffusive transport compared to convective transport and vice versa, and may so affect the observed patterns of sedimentation.

Extensive studies should be made to investigate suspended-sediment compositions, as it is clear that floodplain sedimentation rates and patterns are significantly influenced by sediment type. It is also important to consider studies on characteristics of the deposited sediment (granulometry, porosity, dry weight, etc.), as these are very important parameters to determine the resulting volume of the deposited mass. Further modelling studies could be carried out, to consider the influence of different types of vegetation applied in a uniform manner. This may provide deeper knowledge on the precise effects of each type of vegetation cover on floodplain sedimentation processes, which could be important for future planning scenarios.

ACKNOWLEDGEMENTS

This work was carried out as a part of the Delft Cluster project entitled: 'Safety against flooding'. The authors would like to express their gratitude to Dr E. Mosselman and his colleagues at Deltares, for their valuable comments and their assistance during the modelling phase of this study. Also, to Dr N. Asselman and Dr M. Schoor, for their important collaboration during the data collection phase of the research.

A. Montes Arboleda expresses his gratitude to the Netherlands Fellowship Programme (NUFFIC-NFP) and the Delft Cluster project for the grant that allowed him to carry out the study at UNESCO-IHE Institute for Water Education.

REFERENCES

Asselman NEM. 1997. Suspended sediment in the river Rhine. Netherlands Geographical Studies. PhD thesis, University of Utrecht, Utrecht, The Netherlands, ISBN 90-6266-150-5.

Asselman NEM, Middelkoop H. 1998. Temporal variability of contemporary floodplain sedimentation in the Rhine-Meuse Delta, the Netherlands. *Earth Surface Processes and Landforms* **23**: 595–609.

Bagnold RA. 1966. An approach to the sediment transport problem from general physics. US Geological Survey Paper. 422-I, p. 37.

Baptist MJ. 2005. Modelling Floodplain Biogeomorphology. PhD thesis, Delft University of Technology, Delft, The Netherlands, ISBN 90-407-2582-9.

Baptist MJ, Penning WE, Duel H, Smits AJM, Geerling GW, Lee GEMVD, Alphen JSLV. 2004. Assessment of the effects of cyclic floodplain rejuvenation on flood levels and biodiversity along the Rhine River. *River Research and Applications* **20**: 285–297.

Baptist MJ, Van Den Bosch LV, Dijkstra JT, Kapinga S. 2005. Modelling the effects of vegetation on flow and morphology in rivers. *Archiv für Hydrobiologie Supplement 155/1–4, Large Rivers* **15**(1–4): 339–357.

Baptist MJ, Babovic V, Rodríguez Uthurburu J, Keijzer M, Uittenbogaard RE, Mynett A, Verwey A. 2007. On inducing equations for vegetation resistance. *Journal of Hydraulic Research* **45**(4): 435–450.

Blanckaert K, Glasson L, Jagers HRA, Sloff CJ. 2002. Quasi-3D simulation of flow in sharp open-channel bends with horizontal and developed bed topography. In *Shallow Flows*, Jirka & Uijttewaal W (eds). © Taylor & Francis Group: London, ISBN-90-5809-700-5; 310–315.

Bosch A, Van der Ham W. 1998. *Twee eeuwen Rijkswaterstaat, 1798–1998*. Europese Bibliotheek: Zaltbommel, The Netherlands (In Dutch).

Buijse AD, Coops H, Staras M, Jans LH, Van Geest GJ, Grift RE, Ibelings BW, Oosterbeg W, Roozen FCM. 2002. Restoration strategies for river floodplains along large lowland rivers in Europe. *Freshwater Biology* **47**(4): 867–887. DOI 10.1046/j.1365–2427.2002.00914.x.

Carollo FG, Ferro V, Termini D. 2002. Flow velocity measurements in vegetated channels. *Journal of Hydraulic Engineering* **128**: 664–673.

Corenblit D, Tabacchi E, Steiger J, Gurnell A. 2007. Reciprocal interactions and adjustments between fluvial landforms and vegetation dynamics in river corridors: a review of complementary approaches. *Earth Science Reviews* **84**: 56–86.

Crosato A, Samir-Saleh M. 2010. Numerical study on the effects of floodplain vegetation on reach-scale river morphodynamics. *Earth Surface Processes and Landforms* (in press).

Darby S, Sear D. 2008. *River Restoration. Managing the Uncertainty in Restoring Physical Habitat*. Wiley: Chichester, UK. ISBN 978-0-470-86706-8.

Facchini E, Crosato A, Kater E. 2009. La modellazione numerica nei progetti di riqualificazione fluviale: il caso Ewijkse Plaat, Paesi Bassi. In *Riqualificazione Fluviale, Proceedings of the I° Convegno Italiano sulla Riqualificazione Fluviale*, ECRR-CIRF: Sarzana, 18–19 June 2009, 2/2009, pp. 67–73 (in Italian).

Franz EH, Bazzaz FA. 1977. Simulation of vegetation response to modified hydrologic regimes: a probabilistic model based on niche differentiation in a floodplain forest. *Ecology* **58**: 176–183.

Galappatti R. 1983. *A Depth-Integrated Model for Suspended Transport. Communications on Hydraulics*, No.83-7, Delft University of Technology: Delft, The Netherlands, ISSN 0169–6548.

Galappatti R, Vreugdenhil CB. 1985. A depth-integrated model for suspended sediment transport. *Journal of Hydraulic Research* **23**(4): 359–377.

Hesselink AW. 2002. History makes a river—Morphological changes and human interference in the river Rhine, The Netherlands. Netherlands Geographical Studies. PhD thesis, University of Utrecht, Utrecht, The Netherlands, ISBN 90-6809-327-4.

Hesselink AW, Kleinhans M, Boreel GL. 2006. Historic discharge measurements in three rhine branches. *Journal of Hydraulic Engineering, ASCE* **132**(2): 140–145. DOI: 10.1061/(ASCE)0733–9429.

Hupp CR, Osterkamp WR. 1996. Riparian vegetation and fluvial geomorphic processes. *Geomorphology* **14**: 277–295.

Ikeda S. 1982. Lateral bed slope transport on side slopes. *Journal of Hydraulics Division, ASCE* **108**(11): 1369–1373.

Jeffries R, Darby SE, Sear DA. 2003. The influence of vegetation and organic debris on flood plain sediment dynamics: case study of a low-order stream in the New Forest, England. *Geomorphology* **51**: 61–80.

Johnson WC. 1998. Adjustment of riparian vegetation to river regulation in the Great Plains, USA. *Wetlands* **18**: 608–618.

Klijn F, Dijkman J, Silva W. 2001. Room for the Rhine in the Netherlands. Summary of research results. Report WL Delft Hydraulics Q2975·22, Delft, the Netherlands, ISBN 9036953871.

Lesser GR, Roelvink JA, Van Kester JATM, Stelling GS. 2004. Development and validation of a three dimensional morphological model. *Coastal Engineering* **51**(8–9): 883–915.

Maas GJ, Wolfert HP, Schoor MM, Middelkoop H. 1997. Classificatie van riviertrajecten en kansrijkdom voor ecotopen, Report 552, DLO-Staring Centrum, Wageningen, the Netherlands (in Dutch).

Malmon DV, Dunnet T, Reneau SL. 2002. Predicting the fate of sediment and pollutants in river floodplains. *Environmental Science & Technology* **36**(9): 2026–2032.

Merritt DM, Cooper DJ. 2000. Riparian vegetation and channel change in response to river regulation: a comparative study of regulated and unregulated streams in the Green River Basin, USA. *Regulated Rivers: Research & Management* **16**: 543–564.

Middelkoop H, Asselman NEM. 1998. Spatial variability of floodplain sedimentation at the event scale in the Rhine-Meuse Delta, the Netherlands. *Earth Surface Processes and Landforms* **23**: 561–573.

Middelkoop H. 1997. Embanked floodplains in The Netherlands. Netherlands Geographical Studies. PhD thesis, University of Utrecht, Utrecht, The Netherlands, ISBN 90-6266-146-7.

Middelkoop H. 2002. Reconstructing floodplain sedimentation rates from heavy metal profiles by inverse modelling. *Hydrological Processes* **16**(1): 47–64. DOI: 10.1002/hyp.283.

Piégay H, Darby SE, Mosselman E, Surian N. 2005. A review of techniques available for delimiting the erodible river corridor: a sustainable approach to managing bank erosion. *Rivers Research and Applications* **21**: 773–789. DOI: 10.1002/rra.881.

Pizzuto JE. 1987. Sediment diffussion during overbank flows. *Sedimentology* **34**: 301–317.

Raat AJP. 2001. Ecological rehabilitation of the Dutch part of the River Rhine with special attention to the fish. *Regulated Rivers: Research & Management* **17**(2): 131–144.

Stolker C, Verheij HJ. 2000. Vergelijken van berekeningsmethoden voor de ruwheid van overstroomde flexibele vegetatie. Technical report No. Q2693, WL Delft Hydraulics (DELTARES), Delft, The Netherlands (in Dutch).

Struiksma N, Olesen KW, Flokstra C, De Vriend HJ. 1985. Bed deformation in curved alluvial channels. *Journal of Hydraulic Research, IAHR* **23**(1): 57–79.

Thonon I. 2006. Deposition of sediment and associated heavy metals on floodplains. PhD thesis, University of Utrecht, Utrecht, The Netherlands, ISBN 90-6809-377-0.

Thorne CR. 1990. Effects of vegetation on riverbank erosion and stability. In *Vegetation and Erosion*, Thornes JB (ed.). John Wiley & Sons: Chichester, UK; 125–144.

Tsujimoto T. 1999. Fluvial processes in streams with vegetation. *Journal of Hydraulic Research* **4**(6): 789–803.

Van de Ven GP. 1976. Aan de wieg van Rijkswaterstaat. Wordingsgeschiedenis van het Pannerdens Kanaal. PhD thesis, Nijmegen University, Nijmegen, The Netherlands (In Dutch).

Van Ledden M. 2003. Sand-mud segregation in estuaries and tidal basins. PhD thesis, Delft University of Technology, Delft, the Netherlands, ISBN 90-9016786-2.

Van Velzen EH, Jesse P, Cornelissen P, Coops H. 2003. Stromingsweerstand vegetatie in uiterwaarden; Deel 1 Handboek versie 1–2003 (Tech. Rep. No. 2003·028). Rijkswaterstaat, RIZA (in Dutch).

Villada JA, Crosato A. 2010. Long-term morphological effects of river restoration works including floodplain vegetation: the Common Meuse River—the Netherlands. *I.C.E. Water Management* **163**: 1–11. doi: 10.1680/wama2010.163.1.1.

Van Vuuren W. 2005. Verdeling zomer- en winterhoogwaters voor de Rijntakken in de periode 1770–2004. Memo WRR 2005-012. WRR, The Hague (in Dutch).

Wilson CAME, Stoesser T, Bates PD, Batemann Pinzen A. 2003. Open channel flow through different forms of submerged flexible vegetation. *Journal of Hydraulic Engineering, ASCE* **129**(11): 847–853.

Wu W, Shields FD Jr, Bennet SJ, Wang SSY. 2005. A depth averaged two dimensional model for flow, sediment transport, and bed topography in curved channels with riparian vegetation. *Water Resources Research* **41**: W03015. DOI:10.1029/2004WR003730.

